Occurrence of coexisting dendrite morphologies: Immiscible fluid displacement in an anisotropic radial Hele-Shaw cell under a high flow rate regime

A. G. Banpurkar* and A. V. Limaye†
Center for Advanced Studies in Materials Science, Department of Physics, University of Pune, Pune 411 007, India

S. B. Ogale‡
Department of Physics, University of Maryland, College Park, Maryland 20742

(Received 13 July 1999; revised manuscript received 17 November 1999)

Viscous fingering morphologies during the displacement of a high viscosity fluid by a low viscosity immiscible fluid in a radial fourfold anisotropic Hele-Shaw cell are examined. By using the kerosene-glycerin system for which the μ/T ratio (μ being the relative viscosity and T the interfacial tension between the fluids) is about ten times higher than that for the commonly used air-glycerin system, we have been able to access the hitherto unexplored $N_{ca} \gtrsim 1$ regime (capillary number $N_{ca} = U\mu/T$, U being the advancing fingertip velocity). Within the anisotropy-dominated regime, and when flow rates are significantly high (capillary number well beyond $N_{ca} = 1$), a new phase is seen to evolve wherein the dendrites grow simultaneously along the channels and along the directions making an angle of 45° with the channels, both being kinetically driven. This new phase resembles the one observed in a miscible fluid system at all flow rates of the displacing fluid. [A. G. Banpurkar *et al.*, Phys. Rev. E **59**, 2188 (1999)].

PACS number(s): 68.70.+w, 47.20.Ma, 47.54.+r, 68.10.−m

I. INTRODUCTION

Formation of patterns during nonequilibrium growth processes has always been a subject of considerable research interest in view of the natural appeal of the symmetry of patterns and their occurrence in a wide range of systems [1–7]. Among the various growth systems amenable to laboratory scale experimentation, the phenomenon of viscous fingering is studied in detail due to its vast applicability in commercial and scientific fields, and the simplicity of its experimental demonstration [2,3,7–9]. Viscous fingering is a process in which a low viscosity fluid displaces a high viscosity fluid forming a fingerlike pattern. The Hele-Shaw cell is commonly used for investigation of the viscous fingering in two-dimensional hydrodynamic flows.

Viscous fingering in the Hele-Shaw cell evolves into different morphologies, depending upon various physical parameters, instabilities, and anisotropic effects [1,3,6–20]. Though a definite role of such parameters is not yet fully understood, there are many experiments revealing the manifestation of the interplay of these parameters in the selection of a specific morphology of the patterns [1,3,11–15]. Using an isotropic and an anisotropic radial Hele-Shaw cell, Ben Jacob *et al.* [12,14] have studied this issue in detail. In an anisotropic radial Hele-Shaw cell and using immiscible fluids, the morphology of the patterns evolves through faceted, surface-tension dendrite, tip splitting, and kinetic dendrite morphology, with an increase in the flow rate of the displacing fluid. This evolution of morphological phases is elucidated on the basis of surface tension and kinetic effect. At *very low flow rates*, surface-tension effects are more dominant compared to kinetic effects, which compel the dendrite growth along directions for which the surface area at the interface is minimum. For instance, in the case of the fourfold anisotropic cell, directions making an angle of 45° with the channels are the directions for which surface area at the interface is minimum. Such dendrites are hence termed surface-tension dendrites. While at sufficiently higher flow rates, kinetic effects are much more significant compared to the surface-tension effects. Thus, the most favorable configuration is the one that minimizes the impedance to the flow. In this case, dendrites grow along the channel and are termed kinetic dendrites [14]. For immiscible fluid systems, the kinetic dendrite morphology is the only morphology observed and reported for the high flow rate regime.

Several studies in the Hele-Shaw cell in the high flow rate regime have reported fascinating results [16–20]. In an anisotropic linear Hele-Shaw cell, McCloud *et al.* [16] have observed a larger fingerwidth compared to the Saffman-Taylor (ST) result, when the etched lattice cell size was much smaller compared to the capillary length l, $l = Tb/12\mu U$ (where U is the fingertip velocity, μ is the viscosity of high viscosity fluid, T is the interfacial tension between two fluids, and b is the cell gap) of the flow. In another work performed in an anisotropic linear Hele-Shaw cell, Ben Amar *et al.* [17] have observed that at higher flow rates for which the control parameter $B_1 \to 0$ ($B_1 = Tb^2/12\mu UW^2$, W being a width of the cell), stable and unstable fingers tend to occupy a larger portion of the cell width, which is unusual for the standard ST result. In the case of the isotropic linear Hele-Shaw cell as well, a chaotic and unstable fingering behavior is observed, when the control parameter B_2 ($B_2 = Tb^2/(6(\mu_2+\mu_1)UW^2)$ is made smaller [9,18]. However, all these results are for the linear Hele-Shaw cell, which has its own limitations due to the inherent side wall effects. In another experiment, using a radial isotropic cell, Maxworthy has observed that, for capillary number $N_{ca} \gtrsim 1$ (N_{ca}

*Electronic address: agb@physics.unipune.ernet.in
†Electronic address: avl@physics.unipune.ernet.in
‡Electronic address: ogale@squid.umd.edu

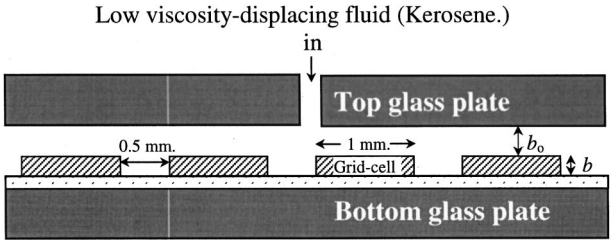

FIG. 1. Schematic (not to the scale) of the anisotropic radial Hele-Shaw cell used in the present work.

$=U\mu/T$), the wavelengths of the most unstable wave for which a growth rate is maximum approaches a value of about five times the cell width [19]. This is very reminiscent of the result of Paterson [20] for the interfacial stability of the miscible fluids, i.e., those for which no surface tension exists. From all these studies, it is seen that an interesting and different physics results at the interface when the capillary length becomes sufficiently small compared to length scales involved in the imposed anisotropy.

The capillary number N_{ca} depends on the interfacial tension between two fluids, viscosity of the high viscous fluid, and fingertip velocity. To reach the interesting regime of $N_{ca} \gtrsim 1$ requires fairly high fingertip velocity for the immiscible fluid systems with small viscosity to surface-tension ratio (μ/T). Hence, in most of the air-liquid systems commonly studied for examining the morphology phase transitions, the regime $N_{ca} \gtrsim 1$ has remained unexplored. Also, in such fluid systems, an effect due to plate flexing prevents the examination of the dendrite morphology at very high flow rates. In the present experiment, these difficulties are overcome by using kerosene as the low viscosity displacing fluid, which forms an immiscible system with glycerine as a high viscosity displaced fluid. The ratio μ/T for the kerosene-glycerine system being considerably higher (about ten times) than that in the case of the air-glycerine system [21], it allows us to reach the regime of $N_{ca} \gtrsim 1$ at relatively low and experimentally accessible flow rates compared to those required in the case of air-glycerine system.

In this work, the morphology of patterns is examined for the immiscible kerosene-glycerine system in an anisotropic radial Hele-Shaw cell for different plate separations b_0 and flow rates. A new phase evolves, wherein dendritic growth occurs simultaneously along the channels and the directions making an angle of 45° with the channels. To the best of our knowledge, this is the first such observation in the case of an immiscible fluid system. Indications of such an occurrence were obtained [Fig. 4(b) of Ref. [1]] and briefly mentioned in our previous paper [1]. That work, however, was primarily focused on the issue of miscible fluids, and the immiscible case was discussed in that paper mainly for the sake of comparison.

II. EXPERIMENT

The experimental anisotropic radial Hele-Shaw cell is comprised of two 1-cm-thick, 30×30 cm^2 float-glass plates. Fourfold anisotropy was introduced by placing a patterned copper circuit board on the horizontal bottom glass plate. The schematic of this cell is shown in Fig. 1. The lattice pattern consisted of a photochemically etched square lattice of copper cells (henceforth referred to as a ''grid cells''). The lateral dimension of the square copper grid cell was 1×1 mm^2, the channel width between the two grid cells was 0.5 mm, and the height of the grid cell b was 0.07 mm. Spacers were used between the copper circuit board and the top glass plate to maintain the desired uniform plate separation b_0. High viscosity glycerine (viscosity 850 cP and surface tension 63 dyn/cm) and low viscosity kerosene (viscosity 1.8 cP and surface tension 28 dyn/cm) were used as the displaced and the displacing fluids, respectively. A tiny amount of blue dye was added in the glycerine for visualization of the patterns. Using an automated fluids delivery system, displacing fluid at constant volumetric flow rate (VFR) was injected through a hole drilled at the center of the top glass plate. The experiments were performed at various values of b_0, ranging from 0.05 to 0.3 mm, and at different values of VFR ranging from 0.06 to 30 ml/min. Fingering patterns were photographed using a CCD camera. A sequence of the images (25 images/sec) was recorded using a VCR. The images were then digitized and computer analyzed.

III. RESULTS AND DISCUSSION

As stated above, the morphologies of a pattern for an immiscible fluid system of kerosene-glycerine were studied at different plate separations b_0 in an anisotropic radial Hele-Shaw cell, for various values of N_{ca}. The variation in the values of N_{ca} was achieved by varying the fingertip velocities. For each value of plate separation b_0, the variation in the fingertip velocities was achieved by performing the experiments at various volume flow rates. The representative picture of the morphologies at various values of N_{ca} and for the plate separation $b_0 = 0.2$ mm is shown in Fig. 2.

In the regime of the lower value of N_{ca}, a changeover from tip-splitting morphology to kinetic dendrite morphology is observed with the increase in the value of N_{ca}. A similar morphology changeover is also observed by other researchers in the case of air-liquid systems [7,14,15]. We wish to point out here that the estimated value of N_{ca} for our lowest flow rate case in Fig. 2, which exhibits tip-splitting morphology, is $N_{ca} \sim 5 \times 10^{-3}$. This is already higher than the regime $N_{ca} \lesssim 10^{-3}$, where surface-tension-type dendrites have been observed [22]. Hence, over the entire flow rate regime in our experiment, if any dendrites are seen at 45° they should not be mistaken with the so-called surface-tension dendrites.

We see from Fig. 2 that in the regime of higher values of N_{ca} (well beyond $N_{ca} = 1$), a new kind of dendritic morphology evolves. In this morphology, a coexistence of kinetic dendrites and the dendrites along the direction 45° to channels is observed. For intermediate values of N_{ca}, an onset of the 45° dendrites is observed along with the kinetic dendrites. However, there is no clear and competitive growth of such 45° dendrites in this regime. In this paper, we focus our attention on the regimes of the kinetic dendrite morphology and its crossover into the evolution of coexisting-dendrite morphology. A consolidated phase diagram of the morphologies is plotted in Fig. 3 as a function of effective anisotropy, Φ [$\Phi = b/(b + b_0)$], and the capillary number N_{ca}. The

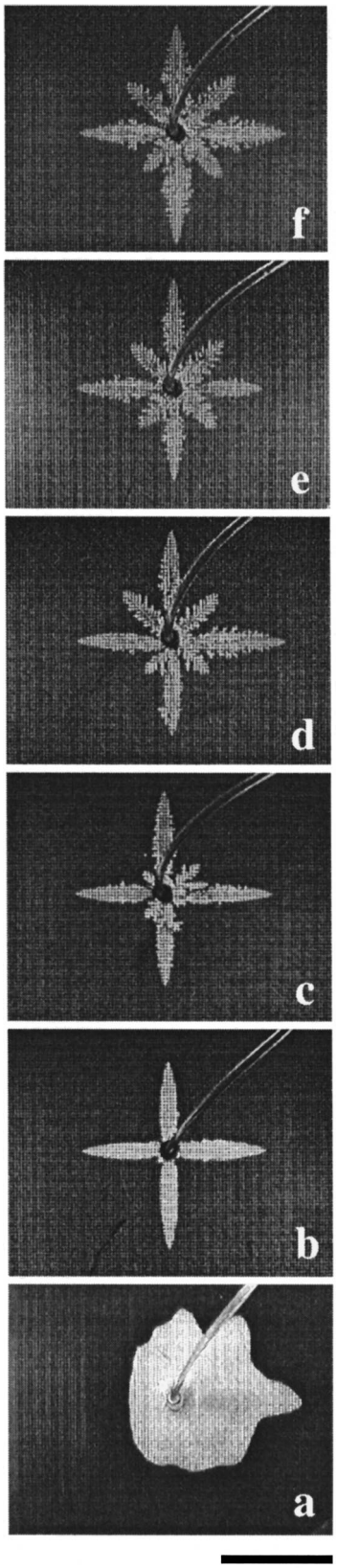

FIG. 2. Morphology of patterns for the $\log_{10}(N_{ca})$ (a) -2.3, (b) -0.05, (c) 0.7, (d) 0.95, (e) 1.2, and (f) 1.3. The plate separation is at $b_0=0.2$ mm (i.e., $\Phi=0.26$) for all cases. The horizontal scale bar is 5 cm long.

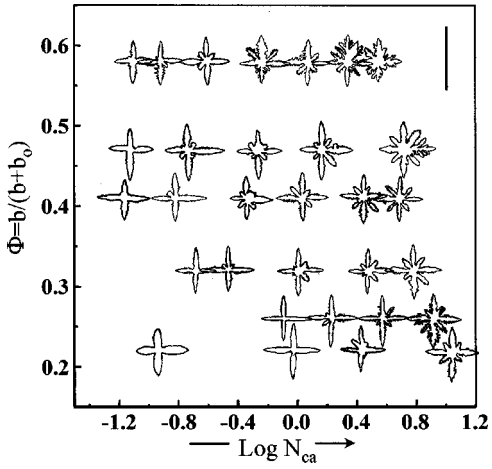

FIG. 3. Consolidated morphology phase diagram for various values of effective anisotropy Φ, and capillary number N_{ca}. The vertical scale bar is 20 cm long.

phase with the coexisting dendrite morphology is observed for the wide range of values of plate separation and in the regime of capillary number well beyond $N_{ca}=1$. It is observed that the morphology changeover from kinetic dendrite to coexisting dendrite morphology is not a sharp transition. Also, from Fig. 3 it is evident that the higher the effective anisotropy, the lower is the value of N_{ca} for which the changeover in the phase takes place.

Interestingly, a similar morphology of coexisting dendrites is observed for a miscible fluid system in an anisotropic radial Hele-Shaw cell for a wide range of flow rates [1]. In light of this work, we have examined in more detail the displacement of immiscible fluid at a microscopic level and have compared it with that for the case of miscible fluid displacement. The zoomed images of a very small region of the pattern for the immiscible system at a representative value of b_0 ($b_0=0.2$ mm) and for two representative values of N_{ca}, namely $N_{ca}=0.2$ and 11.8, are shown in Figs. 4(a) and 4(b), respectively. For the case $N_{ca}<1$ [see Fig. 4(a-1)], the main branch of kinetic dendrite advances through a channel *BCFG*, while a side branch advances along a channel *CFED*. The turning of such a sub-branch towards *EH* is mainly responsible for the growth of the dendrite along a direction of 45° to the channel direction. But this turning is seen to become arrested by the curvature discontinuity at point *E*. Also, as seen from Fig. 4(a-1), this restriction cannot be overcome for the case of $N_{ca}<1$, which in turn results in the evolution of only kinetic-dendrite morphology. On the other hand, for the case $N_{ca}>1$, it is seen from the Fig. 4(b-1) that the sub-branch in the channel *CFED* turns towards *EH* before the whole space *CFED* gets filled up. Also, in contrast to the case of $N_{ca}<1$, the turning of this sub-branch takes place well before the other branch of fluid flow advancing along the channel *AD* joins it. This local behavior of the flow of immiscible fluid for the capillary number $N_{ca}>1$ is quite similar to that for the case of miscible fluids [1]. Hence, in this case also, a new phase with dendrites both along the channels as well as along 45° to the channels evolves, similar to the case of miscible fluids.

For a miscible fluid system, with the absence of any capillary length, there is no abrupt and stable interface between

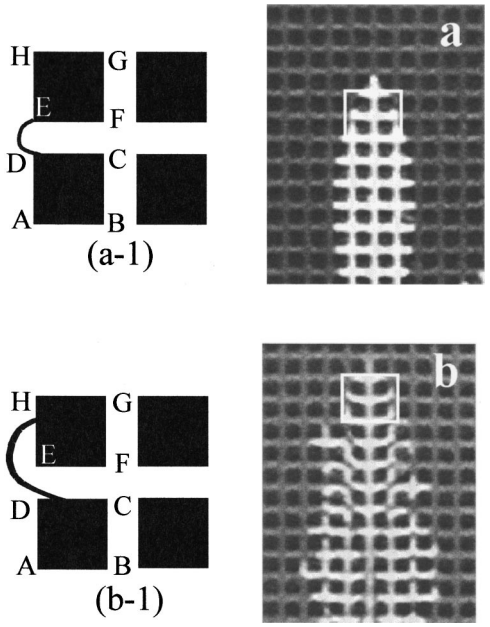

FIG. 4. Zoomed images of the immiscible kerosene-glycerine system for (a) $N_{ca}=0.2$ and (b) $N_{ca}=11.8$. Corresponding schematics of the rectangular regions are given in (a-1) and (b-1). Plate separation in these cases is $b_0=0.2$ mm (i.e., $\Phi=0.26$).

the two fluids. Therefore, the pinning due to the curvature discontinuity at the lattice corners is automatically overcome [1]. As mentioned earlier, immiscible fluid flow has a strikingly similar local behavior and global morphology when capillary number $N_{ca}>1$. Hence, in this immiscible fluid case as well, the surmounting of the curvature discontinuity appears to be the reason for coexisting morphologies for $N_{ca}\gtrsim 1$, although in this case it is kinetically forced.

Maxworthy [19] has emphasized that the three-dimensional nature of the fluid dynamics near the interface is key to the understanding of the evolution of the interface profile in a Hele-Shaw cell, especially for the case of high values of the capillary number N_{ca} for which the viscous forces dissipation begin to dominate over the interfacial tension. The three-dimensional nature embodies the coupling between the evolution of the lateral and vertical profiles of the interface via the tensorial nature of the viscous forces. As Paterson has pointed out, what the flow system will endeavor to achieve under the influence of such forces will be to cause minimum viscous dissipation. In our case, as the fluid protrudes along a side channel (for instance $CFED$), it should have a highly folded interface provide at the corner of a grid cell (say E). This profile would essentially have its central displacing fluid plane advanced much farther than the planes in proximity to the top and bottom plate planes, beyond ED, which may get turned towards EH due to the fluid getting displaced from the channel along AD. The extent of this folding should clearly be an increasing function of N_{ca}. In order to counter the enhanced viscous dissipation resulting from the shear caused by excessive folding, the system will essentially give up on its lateral folding profile above a certain value of N_{ca} by depinning itself from the corner E and forcing itself along the edge EH.

Interestingly, in recent experiments Libbrecht *et al.* [23] have studied electrically induced morphological instabilities in free dendrite growth of ice crystals, where tip velocity increases slowly with the potential. They observed that above a threshold, potential capillarity is insufficient to stabilize growth, which results in a shifted dendrite growth along 30° to the direction of a normal dendrite. Thus, our observation of dendrite growth along the 45° direction (remembering the fourfold symmetry of our case) to that of the kinetic dendrite direction in the case of immiscible fluid at higher fingertip velocities is of special significance in the context of other similar dendrite growth processes. Indeed, this observation has a bearing on the research work in the area of morphological phase diagrams for an immiscible fluid system.

In conclusion, we have studied the morphologies for an immiscible fluid system in an anisotropic radial Hele-Shaw cell for various values of N_{ca}. By using the kerosene-glycerin system for which the μ/T ratio is considerably higher (about ten times) than that in the case of the commonly used air-glycerin system, we have been able to access the $N_{ca}\gtrsim 1$ regime at relatively low and experimentally accessible flow rates. In this regime, a new morphology phase, with kinetic dendrites coexisting with kinetically driven 45° dendrites, is observed.

ACKNOWLEDGMENTS

Two of the authors (A.G.B. and A.V.L.) acknowledge financial assistance from CSIR and DST (Government of India), respectively. One of us (S.B.O.) was supported under NSF-MRSEC Grant No. DMR-96-32521Thanks are also due to Dr. Andrew Schwartz (University of Maryland) for his suggestions towards improvements in the manuscript.

[1] A. G. Banpurkar, A. S. Ogale, A. V. Limaye, and S. B. Ogale, Phys. Rev. E **59**, 2188 (1999).
[2] J. S. Langer, Rev. Mod. Phys. **52**, 1 (1980).
[3] E. Ben-Jacob and P. Garik, Nature (London) **343**, 523 (1990).
[4] E. Ben-Jacob, O. Schochet, A. Tenenbaum, I. Cohen, A. Czirok, and T. Vicsek, Nature (London) **368**, 46 (1994).
[5] O. Zik, Z. Olami, and E. Moses, Phys. Rev. Lett. **81**, 3868 (1998).
[6] M. C. Cross and P. C. Hohenberg, Rev. Mod. Phys. **65**, 851 (1993).
[7] *Fractal Growth Phenomena*, edited by T. Vicsek (World Scientific, New York, 1992).
[8] P. G. Saffman and G. I. Taylor, Proc. R. Soc. London, Ser. A **245**, 312 (1958).
[9] D. Bensimon, L. P. Kadanoff, S. Liang, B. I. Shraiman, and Chao Tang, Rev. Mod. Phys. **58**, 977 (1986).
[10] D. Bonn, H. Kellay, M. Ben Amar, and J. Meunier, Phys. Rev. Lett. **75**, 2132 (1995).
[11] G. Daccord, J. Nittmann, and H. E. Stanley, Phys. Rev. Lett. **56**, 336 (1986).
[12] E. Ben-Jacob, G. Deutscher, P. Garik, N. D. Goldenfeld, and Y. Lareah, Phys. Rev. Lett. **57**, 1903 (1986).
[13] E. Lajeunesse, J. Martin, N. Rakotomalala, and D. Salin, Phys. Rev. Lett. **79**, 5254 (1997).

[14] E. Ben-Jacob, P. Garik, T. Mueller, and D. Grier, Phys. Rev. A **38**, 1370 (1988).
[15] V. Horvath, T. Vicsek, and J. Kertesz, Phys. Rev. A **35**, 2353 (1987).
[16] K. V. McCloud and J. V. Maher, Phys. Rev. E **54**, 1625 (1996).
[17] M. Ben Amar, R. Combescot, and Y. Couder, Phys. Rev. Lett. **70**, 3047 (1993).
[18] J. V. Maher, Phys. Rev. Lett. **54**, 1498 (1985).
[19] T. Maxworthy, Phys. Rev. A **39**, 5863 (1989).
[20] L. Paterson, Phys. Fluids **28**, 26 (1985).
[21] *Principles of Colloid and Surface Chemistry*, edited by Paul C. Hiemenz (Dekker, New York, 1977).
[22] Jordi-Ignes-Mullol and J. V. Maher, Phys. Rev. E **53**, 3788 (1996).
[23] K. G. Libbrecht and V. M. Tanusheva, Phys. Rev. Lett. **81**, 176 (1998).